THE JOURNAL OF BIOLOGICAL CHEMISTRY VOL. 288, NO. 52, pp. 37355–37364, December 27, 2013

A Metabolic Shift Favoring Sphingosine 1-Phosphate at the Expense of Ceramide Controls Glioblastoma Angiogenesis*[S]

Received for publication, June 17, 2013, and in revised form, October 27, 2013 Published, JBC Papers in Press, November 21, 2013, DOI 10.1074/jbc.M113.494740

Hazem J. Abuhusain[‡], Azadeh Matin[§], Qiao Qiao[§], Han Shen[‡], Nupur Kain[§], Bryan W. Day[¶], Brett W. Stringer[¶], Benjamin Daniels[§], Maarit A. Laaksonen[§], Charlie Teo[‖], Kerrie L. McDonald[‡], and Anthony S. Don[§1]

From the [‡]Cure for Life Neuro-oncology Group and [§]Lowy Cancer Research Centre, Prince of Wales Clinical School, Faculty of Medicine, University of New South Wales, Sydney, New South Wales 2052, Australia, the [¶]Brain Cancer Research Unit, Queensland Institute of Medical Research, Brisbane, Queensland 4006, Australia, and the [‖]Centre for Minimally Invasive Neurosurgery, Prince of Wales Private Hospital, Randwick, New South Wales 2033, Australia

Background: The sphingolipid metabolite sphingosine 1-phosphate (S1P) is a potent angiogenic factor.
Results: S1P content is 9-fold higher in glioblastomas compared with normal brain, and S1P production is necessary for glioblastoma cells to trigger endothelial cell angiogenesis.
Conclusion: Excessive S1P synthesis is a major contributor to glioblastoma angiogenesis.
Significance: Inhibiting S1P synthesis may be a valuable antiangiogenic approach in glioblastoma.

Studies in cell culture and mouse models of cancer have indicated that the soluble sphingolipid metabolite sphingosine 1-phosphate (S1P) promotes cancer cell proliferation, survival, invasiveness, and tumor angiogenesis. In contrast, its metabolic precursor ceramide is prodifferentiative and proapoptotic. To determine whether sphingolipid balance plays a significant role in glioma malignancy, we undertook a comprehensive analysis of sphingolipid metabolites in human glioma and normal gray matter tissue specimens. We demonstrate, for the first time, a systematic shift in sphingolipid metabolism favoring S1P over ceramide, which increases with increasing cancer grade. S1P content was, on average, 9-fold higher in glioblastoma tissues compared with normal gray matter, whereas the most abundant form of ceramide in the brain, C18 ceramide, was on average 5-fold lower. Increased S1P content in the tumors was significantly correlated with increased sphingosine kinase 1 (SPHK1) and decreased sphingosine phosphate phosphatase 2 (SGPP2) expression. Inhibition of S1P production by cultured glioblastoma cells, using a highly potent and selective SPHK1 inhibitor, blocked angiogenesis in cocultured endothelial cells without affecting VEGF secretion. Our findings validate the hypothesis that an altered ceramide/S1P balance is an important feature of human cancers and support the development of SPHK1 inhibitors as antiangiogenic agents for cancer therapy.

Gliomas are the most common form of brain tumor in adults. They are classified by the World Health Organization into four grades according to malignancy. Glioblastoma (GBM)[2] is the most common form of glioma, accounting for 12–15% of all intracranial tumors (1). There are approximately 10000 new cases each year in the United States. Despite complete surgical resection followed by cycles of radiotherapy and the DNA-alkylating agent temozolomide, median survival is only 12–15 months, and 5-year survival is less than 10% (1, 2). In an attempt to improve quality of life and survival, targeted therapies are being investigated to augment current treatments. Most have failed to translate into the clinic (3). Recently, the antiangiogenic drug bevacizumab (Avastin), a monoclonal antibody to VEGF, was approved in the United States for patients with recurrent GBM. Bevacizumab improves progression-free survival in GBM, associated with reduced steroid use, but confers little or no improvement in overall survival (4, 5). Most targeted therapies to date are directed against druggable oncogenes identified through genomic profiling. In this study, we investigate lipid metabolism as a potential therapeutic target in GBM.

The sphingolipids are one of the major lipid families in mammalian cells, with a wide range of functions in the organization of cell membranes, cell-cell recognition, and signal transduction (6). The central sphingolipid metabolite is ceramide, to which different head groups may be added, giving rise to a diverse array of lipid and glycolipid structures. Ceramide itself plays an important role in the execution of cell death induced by radiotherapy, chemotherapeutics, lethal autophagy, or proapoptotic TNF family ligands (6–8). These prodeath functions of ceramide are mediated through direct binding to protein targets such as the tumor suppressor phosphatase PP2A (9), kinase suppressor of Ras (10), and autophagy protein LC3B-II (7). Ceramides also play an essential role in neural stem cell differentiation, mediated via direct binding to the kinase PKCζ (8).

* This work was supported by scholarships from the Prince of Wales Clinical School at the University of New South Wales and Cure for Life Foundation (to H. J. A.), by Cancer Institute NSW fellowships (to A. S. D. and K. L. M.), by project grants from Cancer Council NSW (to K. L. M. and A. S. D.) and Cure Cancer Australia (to A. S. D.), by National Health and Medical Research Council project grant APP1024966 (to A. S. D.), and by Cure for Life Foundation funding (to K. L. M.).
[S] This article contains supplemental Table 1.
[1] To whom correspondence should be addressed: Level 2, C25 Lowy Cancer Research Centre, University of New South Wales, Sydney, New South Wales 2052, Australia. Tel.: 61-2-9385-1387; Fax: 61-2-9385-1510; E-mail: anthonyd@unsw.edu.au.

[2] The abbreviations used are: GBM, glioblastoma; HexCer, hexosylceramide; SM, sphingomyelin; NGM, normal gray matter; AII, World Health Organization grade II; AIII, World Health Organization grade III; GNS, glioma neural stem; MTT, 3-(4,5-dimethylthiazol-2-yl)-2,5-diphenyltetrazolium bromide; HBSS, Hanks' buffered salt solution; HMEC, human microvascular endothelial cell.

Ceramide can be catabolized by ceramidases, producing the monoacyl lipid sphingosine. Phosphorylation of sphingosine by sphingosine kinase 1 (SPHK1) or 2 (SPHK2) yields the soluble signaling metabolite sphingosine 1-phosphate (S1P) (Fig. 1*A*). In direct contrast to ceramide, S1P is a potent proliferative, prosurvival, and promigratory factor (11, 12). The majority of the signaling functions of S1P have been attributed to its activation, at low nanomolar potency, of a family of five G protein-coupled receptors, $S1PR_{1-5}$. For example, S1P signaling through $S1P_1$, $S1P_2$, and $S1P_3$ promotes GBM cell invasiveness *in vitro*, mediated through SK1-dependent up-regulation of the urokinase plasminogen activator and its receptor as well as the secreted proinvasive molecule CCN1 (13, 14). However, S1P also binds to and modifies the activity of specific intracellular proteins, such as histone deacetylases, to mediate its effects (11).

The capacity for rapid enzymatic interconversion of ceramide and S1P has given rise to the "sphingolipid rheostat" hypothesis, whereby the balance between prodifferentiative, proapoptotic ceramide and proproliferative, prosurvival S1P exerts a powerful influence over cancer cell fate. This is supported by a large body of data demonstrating an important role for SPHK1 in cellular transformation and cancer progression. SPHK1 overexpression results in oncogenic transformation of normal fibroblasts (15, 16), whereas the absence of SPHK1 in mice protects against the development of colon adenomas (17, 18). Up-regulation of SPHK1 has been observed in many different tumors, including breast (19, 20), lung (21, 22), colon (17, 18), and glioma (23, 24), and increased SPHK1 expression has been associated with a poor survival outcome in GBM (24) as well as breast (20) and lung cancer (22). This has made SPHK1 a target of interest in cancer for biotechnology and pharmaceutical companies.

Despite the implication of SPHK1 in cancer development and malignancy, no studies to date have reported on S1P levels in human cancer tissue specimens. LC-MS/MS now permits the simultaneous quantification of hundreds of lipids, allowing us to take a holistic overview of lipid metabolic pathways. In this study, we quantified levels of S1P, sphingosine, ceramide, hexosylceramide (HexCer), sphingomyelin (SM) and sulfatide in normal gray matter (NGM), diffuse astrocytoma (World Health Organization grade II, AII), anaplastic astrocytoma (World Health Organization grade III, AIII), and GBM (World Health Organization grade IV) tissue specimens. We demonstrate a highly significant shift in the sphingolipid rheostat away from ceramide and in favor of S1P in the tumor tissues that becomes increasingly pronounced as a function of malignancy. Increased S1P content was associated not only with increased SPHK1 expression but also decreased expression of an S1P phosphatase (SGPP2). A highly specific SPHK1 inhibitor, although not affecting GBM cell proliferation, potently inhibits the transfer of angiogenic signals from GBM cells to cocultured endothelial cells.

EXPERIMENTAL PROCEDURES

Clinical Tissue Samples—Cryopreserved and histologically confirmed glioma specimens (AII, AIII, and GBM) were obtained from the Steve and Lynette Waugh Brain Tumor Bank, Centre for Minimally Invasive Neuro-surgery, Prince of Wales Private Hospital, Australia. Enrolment was restricted to treatment-naive tumor specimens. The medical records for all patients were reviewed, and follow-up data were collected. Basic clinical and demographic data collected included age, gender, surgical procedure, treatment received, as well as overall survival. NGM samples were obtained from the New South Wales Tissue Resource Centre, Australian Brain Bank Network. Ethics approval (HREC reference no. 10/174) was from the South Eastern Sydney Illawarra Area Health Service Human Research Ethics Committee.

Sphingolipid Quantification by LC-MS/MS—Lipid extraction and sphingolipid quantification was performed as described previously (25, 26). Sphingomyelins were analyzed separately following an additional alkaline hydrolysis step as described (26, 27). Lipids were quantified relative to external standards for each lipid class as ratios to relevant internal standards: 1250 pmol d18:1/12:0 SM; 250 pmol each of d18:1/12:0 HexCer and d18:1/12:0 sulfatide; and 50 pmol each of d18:1/17:0 ceramide, d17:1 sphingosine, and d17:1 S1P. Lipid content in each sample was then normalized to the tissue mass. Internal and external lipid standards were purchased from Avanti Polar Lipids.

Quantitative Real-time PCR—Total RNA was extracted from all tissue samples using the RNeasy® mini kit (Qiagen GmbH) and converted to cDNA using Superscript™ III First Strand synthesis kit (Invitrogen). An automated pipetting system, epMotion 5075 (Eppendorf), was used to aliquot 5 ng of cDNA template, 0.5 μl of TaqMan probe (Applied Biosystems), 10 μl of TaqMan gene expression master mix (Applied Biosystems), and 5 μl of nuclease-free water into each well. Real-time PCR was performed on an ABI 7900HT (Applied Biosystems) using standard run parameters. The TaqMan probes used were as follows: ACER2 (Hs01892094_g1), ACER3 (Hs00218034_m1), ASAH1 (Hs00602774_m1), ASAH2 (Hs01015655_m1), CERS1 (Hs04195319_s1), CERS2 (Hs00371958_g1), CERS4 (Hs00226114_m1), SGPL1 (Hs00900722_m1), SGPP1 (Hs00229266_m1), SGPP2 (Hs00544786_m1), SPHK1 (Hs00184211_m1), SPHK2 (Hs00219999_m1), 18 S rRNA (4319413E-0909046), and GAPDH (Hs03929097_g1). Each probe was repeated twice for all samples. Expression was quantified from a cDNA standard curve and normalized separately to 18 S rRNA and GAPDH in each sample. Note that there was insufficient tissue to prepare RNA from four of the AII, three of the AIII, and one of the NGM tissue samples used for lipid extraction.

Cell Culture and SK1 Inhibitor Studies—The U87MG cell line was obtained from the ATCC and cultured in minimal essential medium supplemented with 2 mM L-glutamine and 10% FBS. Cells were cultured for a maximum of two months after thawing. The glioma neural stem (GNS) cell lines RN1 and BAH1 have been described recently (28) and were cultured in Neurobasal™ A medium with advanced DMEM/F12 supplemented with 2 mM L-glutamine, B27 supplement, 20 ng/ml bFGF, and 20 ng/ml EGF. Cell culture reagents were purchased from Invitrogen, and growth factors were from Sigma. For GNS cells, culture plates were coated with Matrigel (BD Biosciences) diluted 1:100 in PBS. Cells were seeded at a density of 10^6 cells/10-cm dish to quantify the effect of inhibitors on sphingolipid levels and a density of 500 cells/well in 96-well plates for MTT assays (29). Cell proliferation over time was assayed using an

xCELLigence MP system (Roche Diagnostics). In all experiments, the culture media and inhibitors were replaced every 48 h.

Assessing Cell Viability by Flow Cytometry—Cells were seeded at a density of 5×10^4 cells/well into 12-well plates and incubated for 48 h in growth medium or Hanks' buffered salt solution (HBSS) in the presence of 500 nM SKI-1a, SKI-1b, or dimethyl sulfoxide vehicle control. Cells were dissociated and incubated for 15 min at room temperature with 2% (v/v) annexin V-allophycocyanin (BD Biosciences) and 2.5 μg/ml propidium iodide. Viability was assessed on a BD FACSCanto II flow cytometer.

LC3 Blots—Cells seeded in 12-well plates were preincubated for 24 h with 500 nM SKI-1a or SKI-1b or vehicle control and then incubated for a further 0, 1, 2, 4, or 7 h in HBSS with inhibitors present. Cells were lysed with 0.2 ml radioimmune precipitation assay buffer (10 mM Tris-HCl (pH 7.4), 100 mM NaCl, 1 mM EDTA, 1 mM NaF, 20 mM $Na_4P_2O_7$, 0.1% SDS, 1% TritonX-100, 0.5% sodium deoxycholate, 10% glycerol, and complete protease inhibitor mixture (Roche)). Protein extracts (10 μg) were resolved on 4–12% NU-PAGE gels (Invitrogen) and blotted with anti-LC3 (1:1000, Cell Signaling Technology) followed by anti-rabbit IgG-HRP (1:2000, Cell Signaling Technology). Bands were visualized with Western Lightning Chemiluminescence Reagent Plus (PerkinElmer Life Sciences), imaged with a Fujifilm Las-4000 CCD camera, and quantified by densitometry with Fuji ImageQuant software.

Angiogenesis Assay—The human microvascular endothelial cell line (HMEC-1) was cultured as described previously (30). Angiogenesis was assessed in a three-dimensional fibrin gel coculture model (31). Briefly, near-confluent HMEC-1 cells were incubated with microcarrier beads for 72 h. The microcarriers were then embedded into fibrin gel in 24-well plates, and U87MG cells were seeded on top (25,000 cells/well) in 500 μl of minimal essential medium, 2% FBS, and 2 mM L-glutamine. Medium and compounds were replaced every 48 h, and angiogenic sprouting was assessed after 4 days. Images of 6–10 beads/well were acquired with an AxioVert.A1 inverted microscope (Zeiss). The number and length of angiogenic sprouts was quantified using AxioVision V4.8.2.0 software. Quantification was performed blinded. Conditioned medium for use in this assay was collected from near-confluent U87MG cells cultured for 72 h in minimal essential medium with 2% FBS and 2 mM L-glutamine. To quantify S1P in conditioned medium, 5 ml of cell culture supernatant was centrifuged at 2000 rpm for 5 min to pellet any cells, and the top 4 ml was extracted with an isopropanol/ethyl acetate mixture exactly as described by Bielawski *et al.* (27). S1P was quantified as described above.

Angiogenesis Antibody Arrays—Angiogenesis antibody arrays were purchased from R&D Systems. Angiogenic proteins were detected according to the instructions of the manufacturer using 0.5 ml of cell culture supernatant.

VEGF ELISA—The Quantikine human VEGF ELISA kit from R&D Systems was used to quantify VEGF in cell culture supernatants. Supernatant samples were assayed in duplicate, and the results reported are mean ± S.E. from two separate experiments.

Statistical Analyses—Lipid and gene expression data were log-transformed to create a normal distribution before analysis using one-way analysis of variance. Levene's test was applied to determine whether variances were equal between the different sample groups. When groups displayed equal variances, Tukey's post-test was applied to compare means between different groups. If variances were unequal, Dunnett's T3 post-test was applied. Spearman correlation analysis was used to test for significant correlations between S1P and SPHK1 or SGPP2 expression. Cell culture experiments were analyzed as described in the figure legends.

RESULTS

Gliomas Are Characterized by Decreased Ceramide and Increased S1P—The levels of six related groups of sphingolipids, shown in Fig. 1*A* (ceramide, HexCer, SM, sulfatide, sphingosine, and S1P), comprising 90 individual metabolites, were quantified in NGM, AII, AIII, and GBM tissue samples. Mean metabolite levels in gliomas relative to NGM are shown in Fig. 1*B*. The complete dataset is available in supplemental Table 1. An increase in S1P content (Fig. 1*C*) and a decrease in total ceramides (*D*) with increasing glioma grade was observed. S1P content was, on average, 9-fold higher and total ceramides on average 2-fold lower in GBM than in NGM tissues ($p < 0.001$). Also evident was a loss of the myelin lipids HexCer and sulfatide, which declined by 61 and 66%, respectively, in GBM relative to NGM. There was no significant change in total levels of the most abundant sphingolipid, SM, between NGM and GBM.

Total ceramide content is comprised of multiple distinct ceramide species synthesized by different ceramide synthase enzymes. C18 ceramide (d18:1/18:0 ceramide) was by far the most abundant form in NGM, comprising 69% of the total ceramide mass, and the decrease in total ceramide in the tumor tissue samples can be attributed almost entirely to the loss of C18 ceramide (Fig. 2*A*). The C18 ceramide level was, on average, 5-fold lower in GBM than in NGM ($p < 0.001$). The two next most abundant forms of ceramide, C24:1 ceramide (d18:1/24:1) and C16 (d18:1/16:0), comprising 16 and 6% of total ceramide mass in NGM, respectively, did not decline in the gliomas (Fig. 2, *B* and *C*). Ceramide can be converted to SM or HexCer, or it can be catabolized to sphingosine and subsequently phosphorylated to yield S1P (Fig. 1). C18 SM (d18:1/18:0) was significantly lower in GBM compared with NGM and AII tissues (Fig. 2*D*), and C18 HexCer (d18:1/18:0) trended lower in GBM compared with NGM, although the difference was not statistically significant (*E*). These results indicate that C18 ceramide was not preferentially metabolized to either of these lipids in GBM.

Sphingolipid Enzyme Expression Is Geared toward S1P Production in Glioma—We next determined whether the altered levels of sphingolipid rheostat metabolites were reflected by alterations in the associated gene expression profile. The mRNA levels for genes encoding the enzymes capable of converting ceramide to S1P, and vice versa, were measured in the same tissue samples as were used for metabolite profiling (Fig. 3*A*). In agreement with results published previously (23), SPHK1 expression increased with increasing glioma grade (Fig. 3*B*). The mean expression of SPHK1 was, on average, 7-fold higher in GBM than in NGM tissues and 3-fold higher than in AII samples ($p < 0.001$). There was also a notable decline in

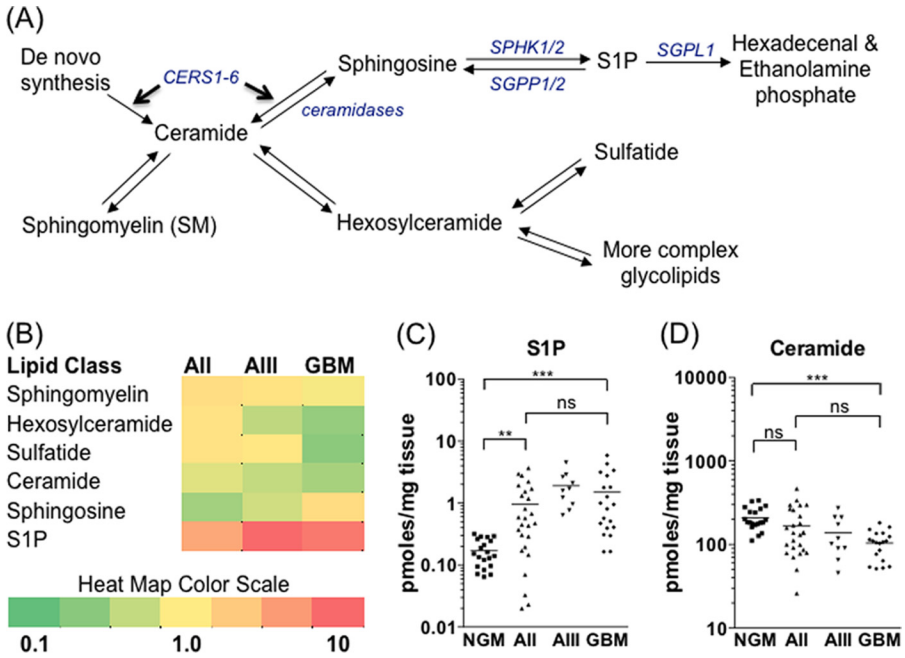

FIGURE 1. **S1P/ceramide balance shifts as a function of glioma malignancy.** *A*, schematic of basic sphingolipid metabolism. Enzymes controlling the balance between ceramide and S1P are shown in *blue italics*. Entry into the pathway occurs through *de novo* synthesis of ceramides by ceramide synthases 1–6 (*CERS1–6*). *B*, heat map showing the relative abundance of different sphingolipid metabolites among the four sample groups: NGM ($n = 20$), AII ($n = 26$), AIII ($n = 10$), and GBM ($n = 20$). Each square is the mean of all samples in that group divided by the mean of the control NGM group. *Red* indicates increased and *green* indicates decreased abundance for each metabolite shown. S1P (*C*) and total ceramide (*D*) levels in individual tissue samples. Statistical significance was tested as described under "Experimental Procedures" (*, $p < 0.05$; **, $p < 0.01$; ***, $p < 0.001$; *ns*, not significant). For clarity of presentation, only significance of comparisons between NGM, AII, and GBM is shown.

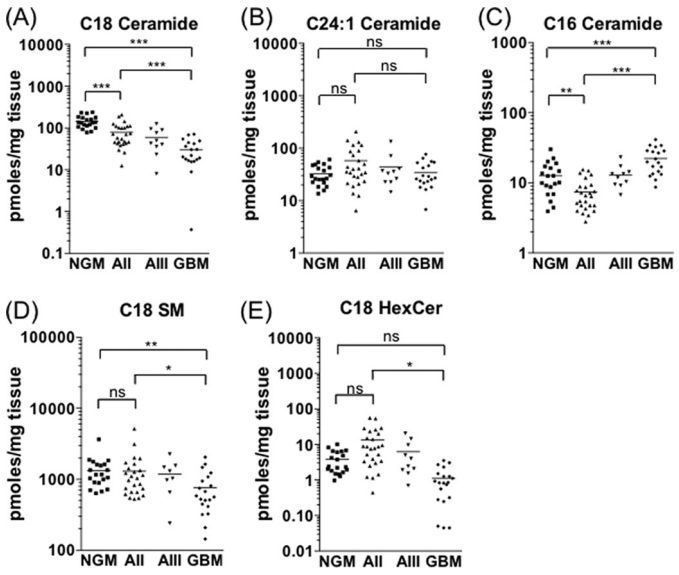

FIGURE 2. **C18 ceramide declines in line with glioma malignancy.** Shown are levels of C18 ceramide (*A*), C24:1 ceramide (*B*), C16 ceramide (*C*), C18 SM (*D*), and C18 hexosylceramide (*E*) in NGM, AII, AIII, and GBM tissue samples. Statistical significance was tested as described under "Experimental Procedures" (*, $p < 0.05$; **, $p < 0.01$; ***, $p < 0.001$; *ns*, not significant).

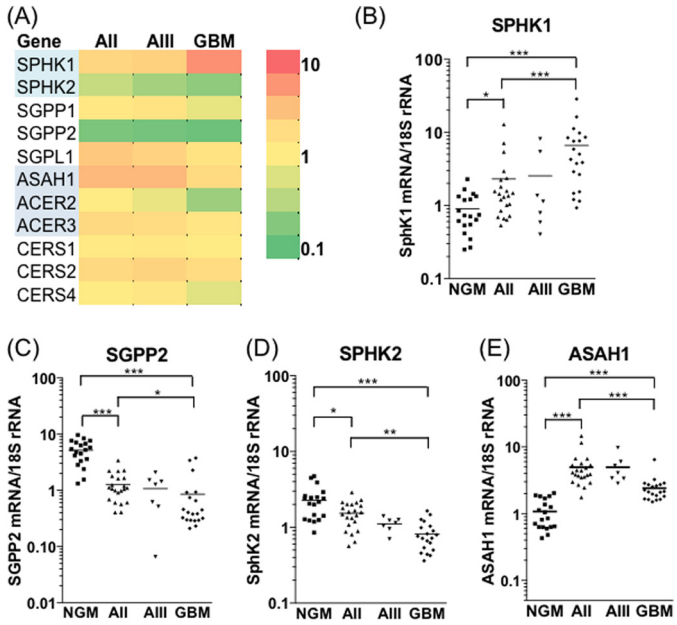

FIGURE 3. **Increased SPHK1 and decreased SGPP2 expression drive S1P production in gliomas.** *A*, heat map showing mRNA expression of enzymes catalyzing reactions that interconvert ceramide, sphingosine, and S1P. Average gene expression levels, normalized to 18 S rRNA, in AII ($n = 22$), AIII ($n = 7$), and GBM ($n = 20$) are expressed as fold changes over the average of 19 NGM samples. *Red* indicates increased and *green* indicates decreased expression. Normalizing enzyme expression to GAPDH gave very similar results for all genes examined. *SGPP1*, sphingosine 1-phosphate phosphatase 1; *SGPL1*, sphingosine 1-phosphate lyase; *ACER2*, alkaline ceramidase 2; *ACER3*, alkaline ceramidase 3; *CERS4*, ceramide synthase 4. *B–E*, expression level for SPHK1 (*B*), SGPP2 (*C*), SPHK2 (*D*), and ASAH1 (*E*) is shown for each sample in the cohort. Statistical significance was tested as described under "Experimental Procedures" (*, $p < 0.05$; **, $p < 0.01$; ***, $p < 0.001$). Expression of neutral ceramidase ASAH2 was below the limit of detection.

expression of the S1P phosphatase SGPP2, which catalyzes the reverse reaction to SPHK1 by dephosphorylating S1P (32). SGPP2 expression was, on average, 6-fold lower in GBM and 4-fold lower in AII compared with NGM (Fig. 3*C*, $p < 0.001$). Accordingly, there was a positive correlation between S1P level and SPHK1 mRNA across all tissue samples ($p = 0.002$, $r = 0.377$) and a strong inverse correlation between SGPP2 expres-

sion and S1P level ($p = 0.0005$, $r = -0.412$). In direct contrast to SPHK1, average SPHK2 expression in GBM tissues was 3-fold lower than in NGM ($p < 0.001$) and 2-fold lower than in AII samples ($p < 0.01$), suggestive of an inverse regulation of these two enzymes (Fig. 3*D*).

C18 ceramide synthesis is catalyzed primarily by CERS1, which is highly abundant in the brain (33, 34). CERS1 expression was unchanged between NGM and the astrocytoma samples, indicating that reduced C18 ceramide levels could not be attributed to the loss of this enzyme. Interestingly, expression of CERS2, the enzyme responsible for formation of very long chain ceramides (33, 35), was, on average, 2.3-, 2.7-, and 2.1-fold higher in AII, AIII, and GBM tissues, respectively, compared with NGM ($p < 0.001$). Acid ceramidase (ASAH1), which converts ceramide to sphingosine, was significantly up-regulated in all gliomas (Fig. 3*E*), although less so in GBM compared with AII and AIII tissues. Increased expression of CERS2 may maintain levels of very long chain ceramides such as C24:1 (Fig. 2*B*) despite increased flux through the ceramidase-SPHK1 pathway. Overall, our metabolite and gene expression results suggest increased flux through the pathway converting ceramide to S1P, with the most significant changes being gain of SPHK1 and loss of SGPP2.

A Highly Specific SPHK1 Inhibitor Does Not Affect GBM Cell Proliferation and Viability—Recently, some controversy over the role of SPHK1 in cancer cell proliferation and survival has arisen, with three independent research teams reporting on highly potent, highly selective SPHK1 inhibitors that do not affect cancer cell proliferation or survival (36–38). In light of our gene expression and metabolite data, we probed the role of S1P overproduction by SPHK1 in GBM cell proliferation and viability using one of these inhibitors, SKI-1a, which has a K_i of 100 nM (36). The stereoisomer, SKI-1b, is two orders of magnitude less potent as a SPHK1 inhibitor and, therefore, acts as a control compound.

In the GBM cell line U87MG, which expresses SPHK1 at high levels (Fig. 4*A*), SKI-1a, but not SKI-1b, dose-dependently reduced S1P levels (*B*). This was coupled to an increase in sphingosine and total ceramide (Fig. 4, *C* and *D*). Despite this, SKI-1a had no effect on U87MG proliferation, assessed using either the MTT assay or the xCELLigence system (Fig. 4, *E* and *F*), or cell viability, assessed by flow cytometry (*G*). SKI-1a did not sensitize these cells to temozolomide (*TMZ*), the standard therapy used for GBM in the clinic (Fig. 4*H*).

Similarly, SKI-1a did not affect proliferation, temozolomide sensitivity, or viability of the primary GNS cell line RN1 (28), which is also characterized by high SPHK1 expression (Fig. 5, *A*–*E*). GNS cells are maintained in serum-free medium supplemented with bFGF and EGF. These conditions accurately preserve the glioblastoma phenotype, resulting in a cell culture model that more closely resembles clinical GBM (39). There was also no effect of SKI-1a on proliferation or viability of the GNS cell line BAH1 (data not shown), which is characterized by lower SPHK1 expression (Fig. 5*A*). SPHK1 has been reported to maintain cell viability under conditions of nutrient deprivation and enhanced autophagy (40). Inhibition of autophagosome turnover with chloroquine, visualized as accumulation of the autophagy marker LC3B-II, indicated active autophagy under growth conditions. A high concentration of SKI-1a (500 nM) did not affect basal autophagy or the modest induction of LC3B-II seen at ~2 h under conditions of nutrient deprivation (Fig. 5*F*). SKI-1a treatment did not sensitize U87MG or RN1 cells to loss of viability caused by culturing under conditions of nutrient deprivation (Figs. 4*G* and 5*E*). In summary, these results indicate that GBM cell proliferation and viability are not directly dependent on bulk S1P production by SPHK1.

SPHK1 Activity Is Necessary for Angiogenic Signaling—S1P has for some time been recognized as a potent angiogenic factor, and a role in tumor angiogenesis has been established using both genetic and pharmacological approaches (41–43). Angiogenesis was examined in a three-dimensional coculture model in which HMEC-1 cells were grown on microcarrier beads embedded in a fibrin gel and formed sprouts in response to angiogenic factors secreted by U87MG cells grown on top of the fibrin gel (Fig. 6*A*). This *in vitro* model closely reproduced all the key features of physiological angiogenesis (31, 44). In the absence of U87MG cells, there was very little sprouting of endothelial cells after 4 days in culture. Addition of U87MG cells promoted endothelial sprouting from the microcarriers, which was dose-dependently inhibited by SKI-1a but not the control compound, 1b (Fig. 6, *A*–*D*). The number of sprouts, average sprout length, and the proportion of long sprouts were reduced at 100 nM and further reduced at 300 nM SKI-1a, correlating well with the concentration needed to block S1P production by U87MG cells (Fig. 4*A*). Importantly, SKI-1a had no effect on HMEC-1 proliferation or viability at concentrations up to 1 μM (Fig. 6*E*). These findings indicate that SPHK1 activity is required for the transfer of angiogenic signals from GBM cells to cocultured endothelial cells.

To test whether SPHK1 activity in the U87MG cells or the HMEC-1 cells, or both, is required for angiogenesis, conditioned medium taken from U87MG cells was added to HMEC-1 cells on microcarriers, and sprouting was assessed after 4 days in the presence or absence of SKI-1a. Treatment of the U87MG cells with 500 nM SKI-1a reduced the S1P concentration in the culture medium by 73% (Fig. 7*A*). Angiogenic sprouting was inhibited in conditioned medium taken from U87MG cells that had been treated with SKI-1a (Fig. 7, *B*–*D*) but not when SKI-1a was added to the assay after collecting conditioned medium from untreated U87MG cells (*E*--*G*). This indicates that SPHK1 activity in GBM, but not endothelial cells, is necessary to induce angiogenic behavior in the coculture system. Endothelial sprouting in conditioned medium taken from U87MG cells treated with SKI-1a was rescued by addition of S1P (Fig. 7, *B*–*D*), strongly suggesting that S1P, secreted into the conditioned medium by GBM cells, is an essential cofactor for endothelial sprouting. In further support of this hypothesis, conditioned medium from U87MG cells treated with SKI-1a or 1b was analyzed for expression of 55 different angiogenic cytokines. Secretion of angiogenic factors, including VEGF, uPA, and IL-8, by the U87MG cells was clearly evident (Fig. 8). However, this was not affected by SKI-1a or 1b treatment. Because VEGF is an important angiogenic factor and a current target in GBM therapy, a VEGF ELISA was used to verify the absence of any change in VEGF levels in the supernatant of U87MG cells treated with SKI-1a. VEGF was present at an average of 1.74 ±

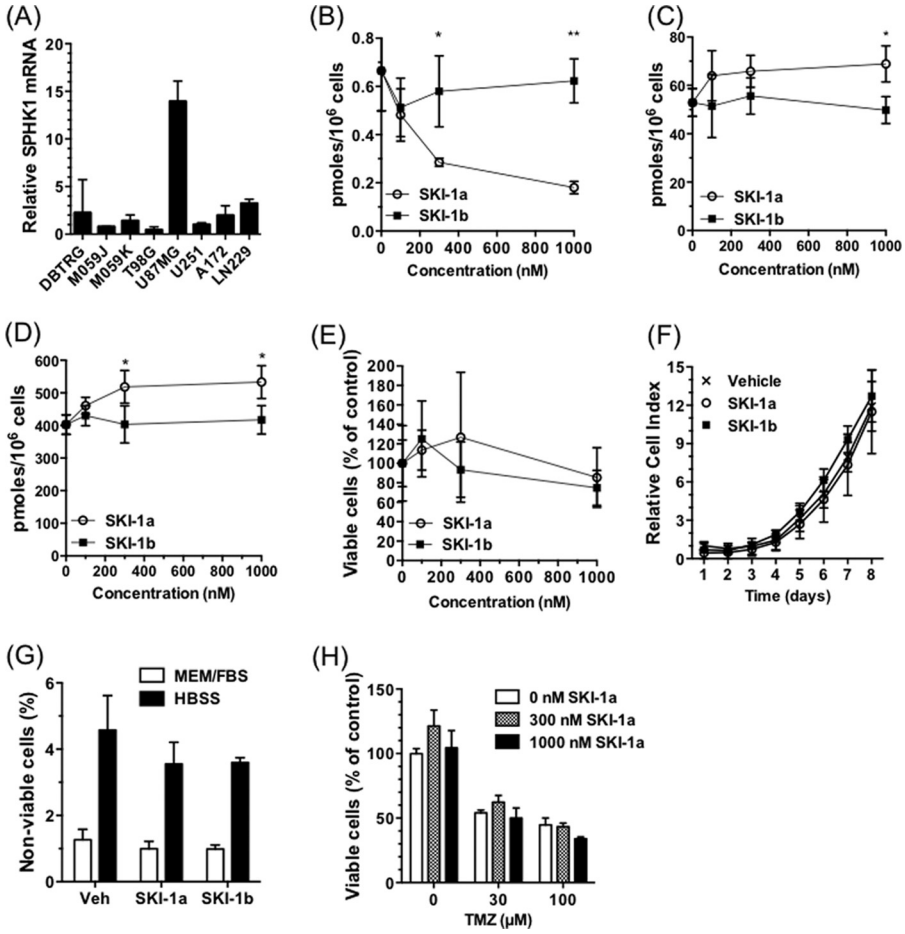

FIGURE 4. **A selective inhibitor of SPHK1 does not affect GBM cell proliferation or survival.** *A*, expression of SPHK1, normalized to 18 S rRNA, was compared in a panel of GBM cell lines. The expression level is relative to the U251 cell line (mean ± S.D. from three measurements). *B–D*, S1P (*B*), sphingosine (*C*), and total ceramide (*D*) content of U87MG cells treated for 72 h with SKI-1a or 1b at the indicated concentrations. Lipids were extracted and quantified as described under "Experimental Procedures." *E*, the effect of SKI-1a and 1b on U87MG cell proliferation was assessed after 7 days by MTT assay. *F*, the effect of 500 nM SKI-1a or 1b on U87MG proliferation was assessed using the xCELLigence real-time growth assay system. *G*, viability of U87MG cells cultured for 48 h in growth medium or HBSS in the presence of 500 nM SKI-1a, SKI-1b, or vehicle control (*Veh*). The proportion of non-viable cells, as detected using annexin V/propidium iodide staining and flow cytometry, is shown. *H*, the effect of SKI-1a on viable U87MG cell number in the presence of the indicated concentrations of temozolomide (*TMZ*) was assessed by MTT assay. Cells were treated for 6 days. Results are mean ± S.D. from a minimum of three treatments and are representative of two experiments. Statistical significance was determined using a two-way analysis of variance followed by Bonferroni's post-test to compare SKI-1a to 1b. *, $p < 0.05$; **, $p < 0.01$; ***, $p < 0.001$.

0.008, 1.63 ± 0.012, and 1.50 ± 0.17 ng/ml supernatant from U87MG cells treated for 48 h with vehicle, 500 nM SKI-1a, or 500 nM SKI-1b, respectively.

DISCUSSION

The hypothesis that cancer cell fate is heavily influenced by the balance between prodifferentiative, proapoptotic ceramide and prosurvival, proangiogenic S1P was first postulated in the 1990s (6, 11, 45). However, few studies have investigated sphingolipid levels in cancer tissue specimens. Our results indicate a metabolic shift in favor of S1P and at the expense of ceramide in human gliomas, suggestive of an increased drive through the pathway converting ceramide to S1P. The magnitude of this metabolic shift increased with increasing malignancy so that it was relatively universal in GBM tissues. All GBMs analyzed had lower C18 ceramide, and 80% had higher S1P, than any of the NGM samples (Figs. 2*A* and 1*C*, respectively). This suggests that these changes to sphingolipid metabolism are independent of the individual genetic fingerprint of each cancer sample, which varies greatly in GBM. Although elevated S1P has been reported in plasma samples from ovarian and breast cancer patients (41, 46), this is the first study to demonstrate increased S1P levels in human cancer tissues.

The sphingolipid profiling results are supported by the gene expression profile, which also points to an increased drive through the pathway converting ceramide to S1P. Numerous studies have described increased SPHK1 expression in a wide array of cancers, including GBM, and have shown that high SPHK1 expression is associated with a poor prognosis (20–24). In addition to SPHK1 up-regulation, we show that the S1P phosphatase SGPP2 is significantly down-regulated in astrocytomas, particularly GBM. Loss of SGPP2 was relatively universal, with 17 of 20 GBM samples having lower SGPP2 expression than any of the NGM samples. The difference in SGPP2 expression between AII and NGM samples was more pronounced than for SPHK1, suggesting that loss of SGPP2 is a major contributor to higher S1P levels in these gliomas. SGPP1 expression has been shown previously to increase ceramide levels by

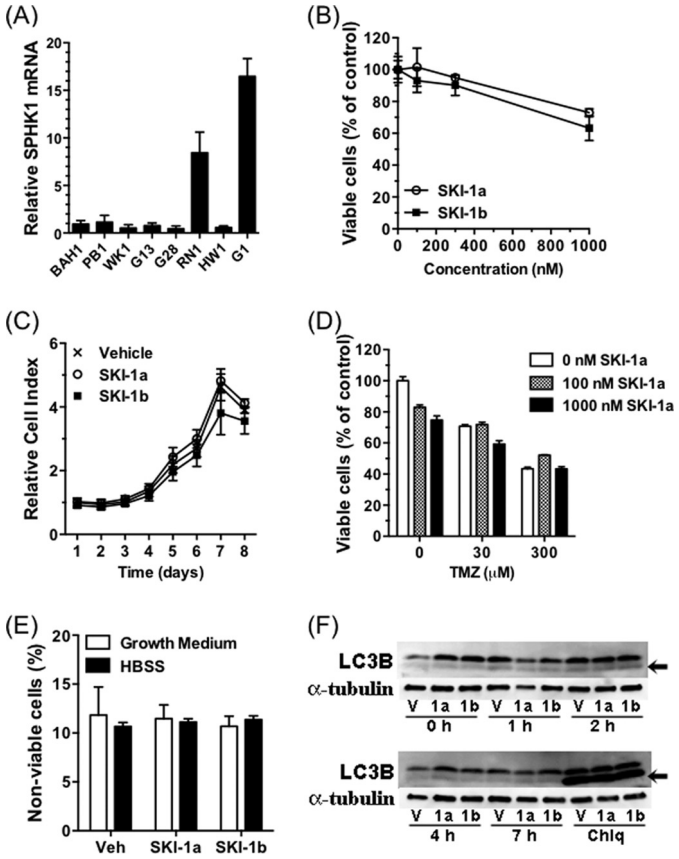

FIGURE 5. **SPHK1 inhibitor SKI-1a does not affect GNS cell proliferation or survival.** *A*, expression of SPHK1, normalized to 18 S rRNA, was compared in a panel of GNS cell lines. The expression level is relative to the BAH1 cell line. *B*, the effect of SKI-1a and 1b on RN1 proliferation was assessed after 7 days by MTT assay. *C*, the effect of 500 nM SKI-1a or 1b on RN1 proliferation was assessed using the xCELLigence real-time growth assay system. *D*, the effect of SKI-1a on viable RN1 cell number after 3 days in the presence of temozolomide (*TMZ*), measured using an MTT assay. *E*, RN1 cells were cultured for 48 h in growth medium or HBSS in the presence of 500 nM SKI-1a, SKI-1b, or vehicle control (*Veh*). The proportion of non-viable cells was determined by flow cytometry. Proliferation and viability results are mean ± S.D. derived from a minimum of three treatments and are representative of two experiments. *F*, RN1 cells were pretreated for 24 h with 500 nM SKI-1a, SKI-1b, or vehicle control and then incubated for the indicated times in HBSS. Lysates were blotted with anti-LC3B, after which the membranes were stripped and reprobed with anti-α-tubulin as a loading control. The *arrows* indicate the lower LC3B-II band, a marker of autophagy. Some wells were treated for 24 h with 10 μM chloroquine (*Chlq*) as a positive control to block autophagosome turnover. *V*, vehicle control.

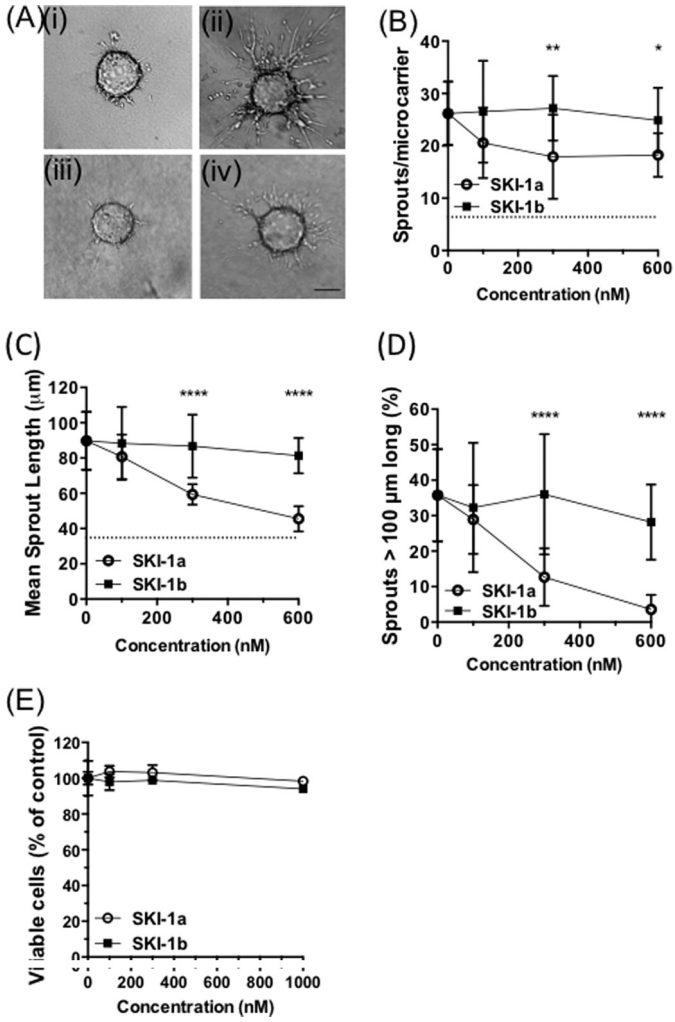

FIGURE 6. **SPHK1 activity is required for *in vitro* angiogenesis.** *A–D*, HMEC-1 cells grown on microcarrier beads were cocultured with U87MG cells, and angiogenic response was assessed after 4 days. *A*, representative images of microcarrier beads in the absence (*i*) or presence (*ii–iv*) of U87MG cells treated with vehicle only (*ii*), 0.3 μM SKI-1a (*iii*), or 0.3 μM SKI-1b (*iv*). *Scale bar* = 100 μm. *B–D*, number of sprouts per microcarrier (*B*), mean length of each sprout (*C*), and percentage of sprouts greater than 100 μm in length (*D*) were determined for a minimum of 10 microcarriers derived from three experimental repeats. Mean ± S.D. are shown for each condition. The base-line values obtained with microcarriers in the absence of cocultured U87MG cells are shown as *dotted lines*. *E*, HMEC-1 cells were treated for 7 days with the indicated concentrations of SKI-1a or 1b, and viable cell number was assessed with an MTT assay (mean ± S.D. from triplicate treatments, representative of two experiments). Statistical significance was determined using a two-way analysis of variance followed by a Bonferroni's post-test to compare SKI-1a to 1b. *, $p < 0.05$; **, $p < 0.01$; ***, $p < 0.001$; ****, $p < 0.0001$.

recycling S1P, formed by SPHK2, into sphingosine and, thence, ceramide at the endoplasmic reticulum (47). Therefore, it is possible that the loss of SGPP2 expression in astrocytomas, potentially in conjunction with decreased SPHK2 expression, drives ceramide levels down. This will be investigated in future studies.

A decline in total ceramides in high-grade *versus* low-grade gliomas, and in gliomas compared with peritumoral tissue, has been demonstrated in a previous study that used a biochemical assay to measure ceramide content (48). Total ceramide content is comprised of multiple distinct ceramide species that cannot be distinguished using these older biochemical approaches but are readily distinguished using LC-MS/MS. In this study, we identify a specific reduction in C18 ceramide as a function of tumor grade. In a study looking specifically at ceramide levels in head and neck squamous cell carcinoma, C18 ceramide was also the only form of ceramide whose levels were decreased, and levels of this metabolite inversely correlated with metastasis (49). CERS1-mediated C18 ceramide synthesis was shown subsequently to induce cell death in head and neck carcinoma cells (50), an effect that appears to result from lethal mitochondrial autophagy (7). Noting that GBM is a distinct disease from the grade II and III astrocytomas used in this study, we hypothesize that reduced C18 ceramide levels may be a common feature in several forms of cancer, contributing to the intrinsic resistance to cell death that is characteristic of cancer cells.

Our results address a significant controversy in current research on SPHK1 and S1P. An abundance of literature using

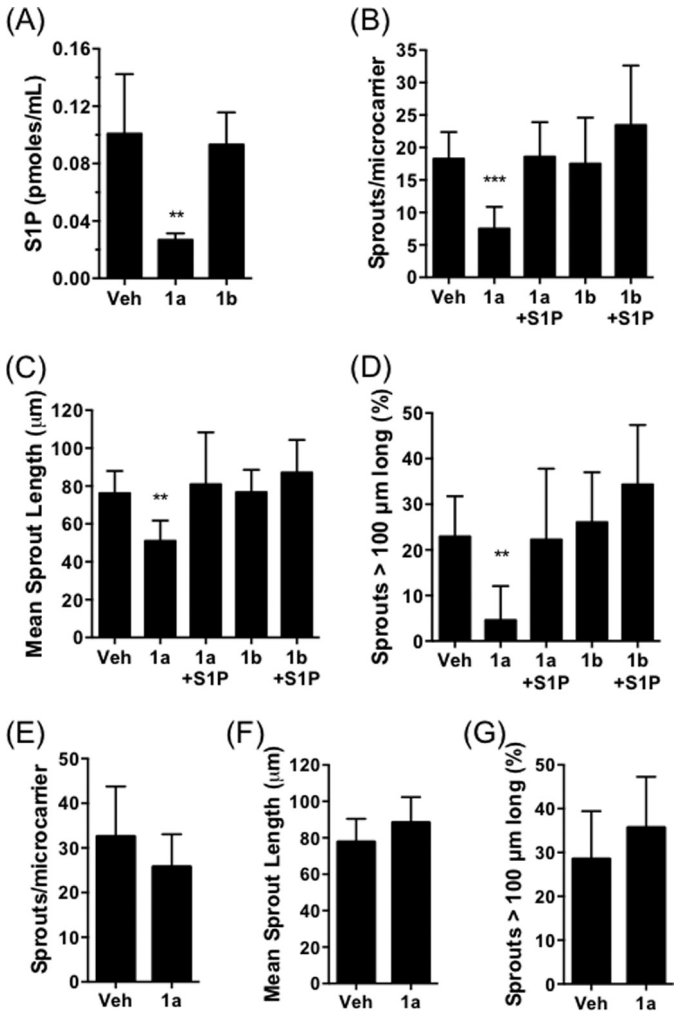

FIGURE 7. **SPHK1-mediated S1P secretion by GBM cells drives *in vitro* angiogenesis.** *A*, S1P concentration in cell culture medium was determined following 72 h treatment of U87MG cells with vehicle (*Veh*), 500 nM SKI-1a (*1a*), or 500 nM SKI-1b (*1b*). Results are mean ± S.D. of four independent treatments. *B–D*, number of sprouts per microcarrier (*B*), mean sprout length (*C*), and percentage of sprouts greater than 100 μm in length (*D*) were determined for HMEC-coated microcarriers cultured for 4 days in conditioned medium taken from U87MG cells treated with vehicle, 500 nM SKI-1a, or 500 nM SKI-1b. S1P (100 nM) was added directly to the angiogenesis assay where indicated. Results shown are mean ± S.D. derived from a minimum of 10 microcarriers/condition and are representative of two independent experiments. Statistical significance was determined using a one-way analysis of variance followed by Dunnett's post-test comparing all treatments to the vehicle control. *, $p < 0.05$, **, $p < 0.01$, ***, $p < 0.001$. *E–G*, number of sprouts per microcarrier (*E*), mean sprout length (*F*), and percentage of sprouts greater than 100 μm in length (*G*) were determined for HMEC-coated microcarriers cultured for 4 days in U87MG cell-conditioned medium and treated with vehicle or 500 nM SKI-1a. None of these measures differed significantly between the vehicle control and SKI-1a, as determined by unpaired *t* tests.

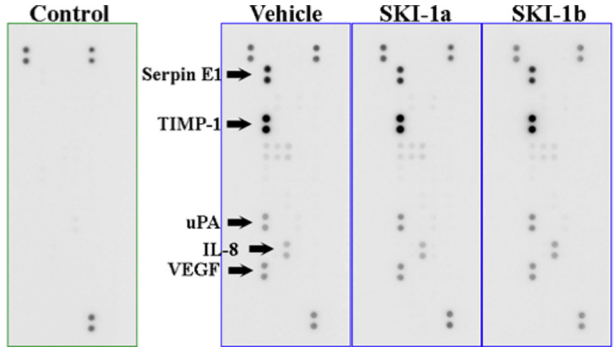

FIGURE 8. **SPHK1 inhibition does not affect secretion of angiogenic cytokines by U87MG cells.** Angiogenesis antibody arrays were probed with conditioned medium taken from U87MG cells incubated for 48 h with 500 nM SKI-1a, SKI-1b, or dimethyl sulfoxide vehicle. The five strongest signals detected on the membrane corresponded to Serpin E1, TIMP-1, uPA, IL-8, and VEGF, as indicated. The control membrane was probed with fresh medium. Positive spots in the control medium are intrinsic controls on each array membrane. No angiogenic cytokines were detected on this membrane.

both genetic ablation and SPHK inhibitors with micromolar inhibitory constants has described a role for SPHK1 in cancer cell proliferation and resistance to radiotherapy and chemotherapeutics (19, 51–53). In agreement with the results published by Kharel *et al.* (36), Schnute *et al.* (37), and Rex *et al.* (38), we found that specific pharmacological inhibition of bulk S1P production by SPHK1 does not affect cancer cell proliferation and therapeutic resistance. However, SKI-1a did inhibit the angiogenic response of cocultured endothelial cells, in agreement with recent results showing an antiangiogenic effect of another SPHK1 inhibitor (41) and an inhibitory effect of SPHK1 silencing in cancer cells on the alignment of cocultured endothelial cells into tube-like structures in the two-dimensional Matrigel angiogenesis model (54). SKI-1a affected the early sprouting response in our experiments, as treatment with this compound elicited a reduction in both the number of sprouts and the length of sprouts, particularly the alignment of endothelial cells into long, multicellular sprouts (Fig. 6*D*).

A number of observations indicate that SKI-1a inhibits endothelial sprouting by blocking the secretion of S1P by GBM cells: 1) S1P in the culture medium of U87MG cells treated with SKI-1a was reduced by 73%; 2) endothelial sprouting was inhibited in conditioned medium taken from GBM cells treated with SKI-1a but not when SKI-1a was added to endothelial cells cultured in conditioned medium from untreated GBM cells; 3) addition of exogenous S1P to conditioned medium taken from GBM cells treated with SKI-1a restored angiogenic sprouting; and 4) secretion of major angiogenic factors, including VEGF, by GBM cells was not affected by SKI-1a treatment. This latter result demonstrates that S1P signaling is required even when potent angiogenic factors such as VEGF are present in the culture medium. An essential role for S1P, signaling through endothelial cell $S1P_1$ receptors, in tumor angiogenesis has been demonstrated previously (43), and an anti-S1P monoclonal antibody has been shown to inhibit tumor angiogenesis (42). The inhibitors used in this study exhibit a very short half-life *in vivo* (36), precluding their use in preclinical mouse models of GBM. It will be of great interest and importance to determine whether future potent and selective SPHK1 inhibitors with an improved pharmacokinetic profile inhibit GBM angiogenesis in mouse models.

In conclusion, the changes to sphingolipid metabolism that we describe in this study are an important confirmation that the ceramide-S1P rheostat is broadly relevant to human cancer tissue. Concomitant up-regulation of SPHK1 and down-regulation of the S1P phosphatase SGPP2 underscores the importance of S1P production in astrocytomas. An order of magnitude increase in the local S1P concentration is very likely to play a key role as a driver of angiogenesis in GBM, which is a highly angiogenic tumor. Anti-VEGF therapies afford an

improvement in quality of life and progression-free survival in GBM but do not significantly enhance overall survival (4, 5). Combining anti-VEGF treatments with inhibition of S1P synthesis could enhance the potency of antiangiogenic therapies in GBM and other highly vascular tumors. Our results, therefore, provide important evidence supporting inhibition of S1P synthesis as a target for antiangiogenic therapy in cancer.

Acknowledgments—We thank Sarita Tiwari and Dr. Russ Pickford for technical assistance and SphynKx Therapeutics LLC, University of Virginia, for the gift of the inhibitors SKI-1a and SKI-1b. We also thank the New South Wales Tissue Resource Centre at the University of Sydney, which is supported by the National Health and Medical Research Council of Australia, the Schizophrenia Research Institute, and National Institute of Alcohol Abuse and Alcoholism, National Institutes of Health Grant R24AA012725 for control brain tissue samples, and acknowledge subsidized access to the Bioanalytical Mass Spectrometry Facility at the University of New South Wales, supported by the National Collaborative Research Infrastructure Scheme.

REFERENCES

1. Wen, P. Y., and Kesari, S. (2008) Malignant gliomas in adults. *N. Engl. J. Med.* **359,** 492–507
2. Stupp, R., Hegi, M. E., Mason, W. P., van den Bent, M. J., Taphoorn, M. J., Janzer, R. C., Ludwin, S. K., Allgeier, A., Fisher, B., Belanger, K., Hau, P., Brandes, A. A., Gijtenbeek, J., Marosi, C., Vecht, C. J., Mokhtari, K., Wesseling, P., Villa, S., Eisenhauer, E., Gorlia, T., Weller, M., Lacombe, D., Cairncross, J. G., Mirimanoff, R. O., European Organisation for Research and Treatment of Cancer Brain Tumour and Radiation Oncology Groups, and National Cancer Institute of Canada Clinical Trials Group (2009) Effects of radiotherapy with concomitant and adjuvant temozolomide versus radiotherapy alone on survival in glioblastoma in a randomised phase III study: 5-year analysis of the EORTC-NCIC trial. *Lancet Oncol.* **10,** 459–466
3. Bai, R. Y., Staedtke, V., and Riggins, G. J. (2011) Molecular targeting of glioblastoma. Drug discovery and therapies. *Trends Mol. Med.* **17,** 301–312
4. Lai, A., Tran, A., Nghiemphu, P. L., Pope, W. B., Solis, O. E., Selch, M., Filka, E., Yong, W. H., Mischel, P. S., Liau, L. M., Phuphanich, S., Black, K., Peak, S., Green, R. M., Spier, C. E., Kolevska, T., Polikoff, J., Fehrenbacher, L., Elashoff, R., and Cloughesy, T. (2011) Phase II study of bevacizumab plus temozolomide during and after radiation therapy for patients with newly diagnosed glioblastoma multiforme. *J. Clin. Oncol.* **29,** 142–148
5. Friedman, H. S., Prados, M. D., Wen, P. Y., Mikkelsen, T., Schiff, D., Abrey, L. E., Yung, W. K., Paleologos, N., Nicholas, M. K., Jensen, R., Vredenburgh, J., Huang, J., Zheng, M., and Cloughesy, T. (2009) Bevacizumab alone and in combination with irinotecan in recurrent glioblastoma. *J. Clin. Oncol.* **27,** 4733–4740
6. Hannun, Y. A., and Obeid, L. M. (2008) Principles of bioactive lipid signalling. Lessons from sphingolipids. *Nat. Rev. Mol. Cell Biol.* **9,** 139–150
7. Sentelle, R. D., Senkal, C. E., Jiang, W., Ponnusamy, S., Gencer, S., Selvam, S. P., Ramshesh, V. K., Peterson, Y. K., Lemasters, J. J., Szulc, Z. M., Bielawski, J., and Ogretmen, B. (2012) Ceramide targets autophagosomes to mitochondria and induces lethal mitophagy. *Nat. Chem. Biol.* **8,** 831–838
8. Bieberich, E. (2008) Ceramide signaling in cancer and stem cells. *Future Lipidol.* **3,** 273–300
9. Chalfant, C. E., Szulc, Z., Roddy, P., Bielawska, A., and Hannun, Y. A. (2004) The structural requirements for ceramide activation of serine-threonine protein phosphatases. *J. Lipid Res.* **45,** 496–506
10. Zhang, Y., Yao, B., Delikat, S., Bayoumy, S., Lin, X. H., Basu, S., McGinley, M., Chan-Hui, P. Y., Lichenstein, H., and Kolesnick, R. (1997) Kinase suppressor of Ras is ceramide-activated protein kinase. *Cell* **89,** 63–72
11. Maceyka, M., Harikumar, K. B., Milstien, S., and Spiegel, S. (2012) Sphingosine-1-phosphate signaling and its role in disease. *Trends Cell Biol.* **22,** 50–60
12. Rosen, H., Gonzalez-Cabrera, P. J., Sanna, M. G., and Brown, S. (2009) Sphingosine 1-phosphate receptor signaling. *Annu. Rev. Biochem.* **78,** 743–768
13. Young, N., and Van Brocklyn, J. R. (2007) Roles of sphingosine-1-phosphate (S1P) receptors in malignant behavior of glioma cells. Differential effects of S1P2 on cell migration and invasiveness. *Exp. Cell Res.* **313,** 1615–1627
14. Young, N., Pearl, D. K., and Van Brocklyn, J. R. (2009) Sphingosine-1-phosphate regulates glioblastoma cell invasiveness through the urokinase plasminogen activator system and CCN1/Cyr61. *Mol. Cancer Res.* **7,** 23–32
15. Xia, P., Gamble, J. R., Wang, L., Pitson, S. M., Moretti, P. A., Wattenberg, B. W., D'Andrea, R. J., and Vadas, M. A. (2000) An oncogenic role of sphingosine kinase. *Curr. Biol.* **10,** 1527–1530
16. Pitson, S. M., Xia, P., Leclercq, T. M., Moretti, P. A., Zebol, J. R., Lynn, H. E., Wattenberg, B. W., and Vadas, M. A. (2005) Phosphorylation-dependent translocation of sphingosine kinase to the plasma membrane drives its oncogenic signalling. *J. Exp. Med.* **201,** 49–54
17. Kawamori, T., Kaneshiro, T., Okumura, M., Maalouf, S., Uflacker, A., Bielawski, J., Hannun, Y. A., and Obeid, L. M. (2009) Role for sphingosine kinase 1 in colon carcinogenesis. *FASEB J.* **23,** 405–414
18. Kohno, M., Momoi, M., Oo, M. L., Paik, J. H., Lee, Y. M., Venkataraman, K., Ai, Y., Ristimaki, A. P., Fyrst, H., Sano, H., Rosenberg, D., Saba, J. D., Proia, R. L., and Hla, T. (2006) Intracellular role for sphingosine kinase 1 in intestinal adenoma cell proliferation. *Mol. Cell Biol.* **26,** 7211–7223
19. French, K. J., Schrecengost, R. S., Lee, B. D., Zhuang, Y., Smith, S. N., Eberly, J. L., Yun, J. K., and Smith, C. D. (2003) Discovery and evaluation of inhibitors of human sphingosine kinase. *Cancer Res.* **63,** 5962–5969
20. Ruckhäberle, E., Rody, A., Engels, K., Gaetje, R., von Minckwitz, G., Schiffmann, S., Grösch, S., Geisslinger, G., Holtrich, U., Karn, T., and Kaufmann, M. (2008) Microarray analysis of altered sphingolipid metabolism reveals prognostic significance of sphingosine kinase 1 in breast cancer. *Breast Cancer Res. Treat.* **112,** 41–52
21. Johnson, K. R., Johnson, K. Y., Crellin, H. G., Ogretmen, B., Boylan, A. M., Harley, R. A., and Obeid, L. M. (2005) Immunohistochemical distribution of sphingosine kinase 1 in normal and tumor lung tissue. *J. Histochem. Cytochem.* **53,** 1159–1166
22. Song, L., Xiong, H., Li, J., Liao, W., Wang, L., Wu, J., and Li, M. (2011) Sphingosine kinase-1 enhances resistance to apoptosis through activation of PI3K/Akt/NF-κB pathway in human non-small cell lung cancer. *Clin. Cancer Res.* **17,** 1839–1849
23. Li, J., Guan, H. Y., Gong, L. Y., Song, L. B., Zhang, N., Wu, J., Yuan, J., Zheng, Y. J., Huang, Z. S., and Li, M. (2008) Clinical significance of sphingosine kinase-1 expression in human astrocytomas progression and overall patient survival. *Clin. Cancer Res.* **14,** 6996–7003
24. Van Brocklyn, J. R., Jackson, C. A., Pearl, D. K., Kotur, M. S., Snyder, P. J., and Prior, T. W. (2005) Sphingosine kinase-1 expression correlates with poor survival of patients with glioblastoma multiforme. Roles of sphingosine kinase isoforms in growth of glioblastoma cell lines. *J. Neuropathol. Exp. Neurol.* **64,** 695–705
25. Wong, J. W., Abuhusain, H. J., McDonald, K. L., and Don, A. S. (2012) MMSAT. Automated quantification of metabolites in selected reaction monitoring experiments. *Anal. Chem.* **84,** 470–474
26. Hejazi, L., Wong, J. W., Cheng, D., Proschogo, N., Ebrahimi, D., Garner, B., and Don, A. S. (2011) Mass and relative elution time profiling. Two-dimensional analysis of sphingolipids in Alzheimer's disease brains. *Biochem. J.* **438,** 165–175
27. Bielawski, J., Szulc, Z. M., Hannun, Y. A., and Bielawska, A. (2006) Simultaneous quantitative analysis of bioactive sphingolipids by high-performance liquid chromatography-tandem mass spectrometry. *Methods* **39,** 82–91
28. Day, B. W., Stringer, B. W., Al-Ejeh, F., Ting, M. J., Wilson, J., Ensbey, K. S., Jamieson, P. R., Bruce, Z. C., Lim, Y. C., Offenhäuser, C., Charmsaz, S., Cooper, L. T., Ellacott, J. K., Harding, A., Leveque, L., Inglis, P., Allan, S., Walker, D. G., Lackmann, M., Osborne, G., Khanna, K. K., Reynolds, B. A., Lickliter, J. D., and Boyd, A. W. (2013) EphA3 maintains tumorigenicity

and is a therapeutic target in glioblastoma multiforme. *Cancer Cell* **23,** 238–248
29. Jary, E., Bee, T., Walker, S. R., Chung, S. K., Seo, K. C., Morris, J. C., and Don, A. S. (2010) Elimination of a hydroxyl group in FTY720 dramatically improves the phosphorylation rate. *Mol. Pharmacol.* **78,** 685–692
30. Ades, E. W., Candal, F. J., Swerlick, R. A., George, V. G., Summers, S., Bosse, D. C., and Lawley, T. J. (1992) HMEC-1. Establishment of an immortalized human microvascular endothelial cell line. *J. Invest. Dermatol.* **99,** 683–690
31. Chen, Z., Htay, A., Dos Santos, W., Gillies, G. T., Fillmore, H. L., Sholley, M. M., and Broaddus, W. C. (2009) *In vitro* angiogenesis by human umbilical vein endothelial cells (HUVEC) induced by three-dimensional co-culture with glioblastoma cells. *J. Neurooncol.* **92,** 121–128
32. Ogawa, C., Kihara, A., Gokoh, M., and Igarashi, Y. (2003) Identification and characterization of a novel human sphingosine-1-phosphate phosphohydrolase, hSPP2. *J. Biol. Chem.* **278,** 1268–1272
33. Mizutani, Y., Kihara, A., and Igarashi, Y. (2005) Mammalian Lass6 and its related family members regulate synthesis of specific ceramides. *Biochem. J.* **390,** 263–271
34. Ginkel, C., Hartmann, D., vom Dorp, K., Zlomuzica, A., Farwanah, H., Eckhardt, M., Sandhoff, R., Degen, J., Rabionet, M., Dere, E., Dörmann, P., Sandhoff, K., and Willecke, K. (2012) Ablation of neuronal ceramide synthase 1 in mice decreases ganglioside levels and expression of myelin-associated glycoprotein in oligodendrocytes. *J. Biol. Chem.* **287,** 41888–41902
35. Laviad, E. L., Albee, L., Pankova-Kholmyansky, I., Epstein, S., Park, H., Merrill, A. H., Jr., and Futerman, A. H. (2008) Characterization of ceramide synthase 2. Tissue distribution, substrate specificity, and inhibition by sphingosine 1-phosphate. *J. Biol. Chem.* **283,** 5677–5684
36. Kharel, Y., Mathews, T. P., Gellett, A. M., Tomsig, J. L., Kennedy, P. C., Moyer, M. L., Macdonald, T. L., and Lynch, K. R. (2011) Sphingosine kinase type 1 inhibition reveals rapid turnover of circulating sphingosine 1-phosphate. *Biochem. J.* **440,** 345–353
37. Schnute, M. E., McReynolds, M. D., Kasten, T., Yates, M., Jerome, G., Rains, J. W., Hall, T., Chrencik, J., Kraus, M., Cronin, C. N., Saabye, M., Highkin, M. K., Broadus, R., Ogawa, S., Cukyne, K., Zawadzke, L. E., Peterkin, V., Iyanar, K., Scholten, J. A., Wendling, J., Fujiwara, H., Nemirovskiy, O., Wittwer, A. J., and Nagiec, M. M. (2012) Modulation of cellular S1P levels with a novel, potent and specific inhibitor of sphingosine kinase-1. *Biochem. J.* **444,** 79–88
38. Rex, K., Jeffries, S., Brown, M. L., Carlson, T., Coxon, A., Fajardo, F., Frank, B., Gustin, D., Kamb, A., Kassner, P. D., Li, S., Li, Y., Morgenstern, K., Plant, M., Quon, K., Ruefli-Brasse, A., Schmidt, J., Swearingen, E., Walker, N., Wang, Z., Watson, J. E., Wickramasinghe, D., Wong, M., Xu, G., and Wesche, H. (2013) Sphingosine kinase activity is not required for tumor cell viability. *PLoS ONE* **8,** e68328
39. Lee, J., Kotliarova, S., Kotliarov, Y., Li, A., Su, Q., Donin, N. M., Pastorino, S., Purow, B. W., Christopher, N., Zhang, W., Park, J. K., and Fine, H. A. (2006) Tumor stem cells derived from glioblastomas cultured in bFGF and EGF more closely mirror the phenotype and genotype of primary tumors than do serum-cultured cell lines. *Cancer Cell* **9,** 391–403
40. Lavieu, G., Scarlatti, F., Sala, G., Carpentier, S., Levade, T., Ghidoni, R., Botti, J., and Codogno, P. (2006) Regulation of autophagy by sphingosine kinase 1 and its role in cell survival during nutrient starvation. *J. Biol. Chem.* **281,** 8518–8527
41. Nagahashi, M., Ramachandran, S., Kim, E. Y., Allegood, J. C., Rashid, O. M., Yamada, A., Zhao, R., Milstien, S., Zhou, H., Spiegel, S., and Takabe, K. (2012) Sphingosine-1-phosphate produced by sphingosine kinase 1 promotes breast cancer progression by stimulating angiogenesis and lymphangiogenesis. *Cancer Res.* **72,** 726–735
42. Visentin, B., Vekich, J. A., Sibbald, B. J., Cavalli, A. L., Moreno, K. M., Matteo, R. G., Garland, W. A., Lu, Y., Yu, S., Hall, H. S., Kundra, V., Mills, G. B., and Sabbadini, R. A. (2006) Validation of an anti-sphingosine-1-phosphate antibody as a potential therapeutic in reducing growth, invasion, and angiogenesis in multiple tumor lineages. *Cancer Cell* **9,** 225–238
43. Chae, S. S., Paik, J. H., Furneaux, H., and Hla, T. (2004) Requirement for sphingosine 1-phosphate receptor-1 in tumor angiogenesis demonstrated by *in vivo* RNA interference. *J. Clin. Invest.* **114,** 1082–1089
44. Nakatsu, M. N., and Hughes, C. C. (2008) An optimized three-dimensional *in vitro* model for the analysis of angiogenesis. *Methods Enzymol.* **443,** 65–82
45. Cuvillier, O., Pirianov, G., Kleuser, B., Vanek, P. G., Coso, O. A., Gutkind, S., and Spiegel, S. (1996) Suppression of ceramide-mediated programmed cell death by sphingosine-1-phosphate. *Nature* **381,** 800–803
46. Sutphen, R., Xu, Y., Wilbanks, G. D., Fiorica, J., Grendys, E. C., Jr., LaPolla, J. P., Arango, H., Hoffman, M. S., Martino, M., Wakeley, K., Griffin, D., Blanco, R. W., Cantor, A. B., Xiao, Y. J., and Krischer, J. P. (2004) Lysophospholipids are potential biomarkers of ovarian cancer. *Cancer Epidemiol. Biomark. Prev.* **13,** 1185–1191
47. Le Stunff, H., Giussani, P., Maceyka, M., Lépine, S., Milstien, S., and Spiegel, S. (2007) Recycling of sphingosine is regulated by the concerted actions of sphingosine-1-phosphate phosphohydrolase 1 and sphingosine kinase 2. *J. Biol. Chem.* **282,** 34372–34380
48. Riboni, L., Campanella, R., Bassi, R., Villani, R., Gaini, S. M., Martinelli-Boneschi, F., Viani, P., and Tettamanti, G. (2002) Ceramide levels are inversely associated with malignant progression of human glial tumors. *Glia* **39,** 105–113
49. Karahatay, S., Thomas, K., Koybasi, S., Senkal, C. E., Elojeimy, S., Liu, X., Bielawski, J., Day, T. A., Gillespie, M. B., Sinha, D., Norris, J. S., Hannun, Y. A., and Ogretmen, B. (2007) Clinical relevance of ceramide metabolism in the pathogenesis of human head and neck squamous cell carcinoma (HNSCC). Attenuation of C(18)-ceramide in HNSCC tumors correlates with lymphovascular invasion and nodal metastasis. *Cancer Lett.* **256,** 101–111
50. Senkal, C. E., Ponnusamy, S., Bielawski, J., Hannun, Y. A., and Ogretmen, B. (2010) Antiapoptotic roles of ceramide-synthase-6-generated C16-ceramide via selective regulation of the ATF6/CHOP arm of ER-stress-response pathways. *FASEB J.* **24,** 296–308
51. Kapitonov, D., Allegood, J. C., Mitchell, C., Hait, N. C., Almenara, J. A., Adams, J. K., Zipkin, R. E., Dent, P., Kordula, T., Milstien, S., and Spiegel, S. (2009) Targeting sphingosine kinase 1 inhibits Akt signaling, induces apoptosis, and suppresses growth of human glioblastoma cells and xenografts. *Cancer Res.* **69,** 6915–6923
52. Endo, K., Igarashi, Y., Nisar, M., Zhou, Q. H., and Hakomori, S. (1991) Cell membrane signaling as target in cancer therapy. Inhibitory effect of *N,N*-dimethyl and *N,N,N*-trimethyl sphingosine derivatives on *in vitro* and *in vivo* growth of human tumor cells in nude mice. *Cancer Res.* **51,** 1613–1618
53. Pchejetski, D., Golzio, M., Bonhoure, E., Calvet, C., Doumerc, N., Garcia, V., Mazerolles, C., Rischmann, P., Teissié, J., Malavaud, B., and Cuvillier, O. (2005) Sphingosine kinase-1 as a chemotherapy sensor in prostate adenocarcinoma cell and mouse models. *Cancer Res.* **65,** 11667–11675
54. Anelli, V., Gault, C. R., Snider, A. J., and Obeid, L. M. (2010) Role of sphingosine kinase-1 in paracrine/transcellular angiogenesis and lymphangiogenesis *in vitro*. *FASEB J.* **24,** 2727–2738